The present results demonstrate that the normalized wake growth behind a solid strip is much faster than behind a porous strip with $\beta = 0.425$. According to the findings of Castro, the wake of the solid strip is dominated by a vortex street which does not form behind the $\beta = 0.425$ porous strip. Taken together, these results indicate that the two-dimensional far wake does depend on the shape of the wake producing object insofar as the shape affects the formation of large vortical structures.

Acknowledgments

The authors gratefully acknowledge the advice of Dr. Paul M. Bevilaqua and thank Prof. Paul S. Lykoudis, Prof. Gerrit H. Toebes, and David L. Cochran for their assistance.

References

[1] Bevilaqua, P. M. and Lykoudis, P. S., "Turbulence Memory in Self-Preserving Wakes," *Journal of Fluid Mechanics*, Vol. 89, Dec. 1978, pp. 589-606.

[2] Hinze, J. O., *Turbulence*, 2nd Ed., McGraw-Hill, New York, 1975, pp. 483-520.

[3] Townsend, A. A., *The Structure of Turbulent Shear Flow*, 2nd Ed., Cambridge University Press, Cambridge, 1976, Chap. 6.

[4] Bevilaqua, P. M. and Lykoudis, P. S., "Entrainment and the Large Eddy Structure," AIAA Paper 75-115, 1975.

[5] Bevilaqua, P. M., personal communication, Aug. 6, 1980.

[6] Brown, G. L. and Roshko, A., "Effect of Density Differences on the Turbulent Mixing Layer," *Turbulent Shear Flows, AGARD Conference Proceedings No. 93*, Paper 23, pp. 1-12.

[7] Papailiou, D. D. and Lykoudis, P. S., "Turbulent Vortex Streets and the Mechanism of Entrainment," *Journal of Fluid Mechanics*, Vol. 62, Jan. 1974, pp. 11-31.

[8] Hwang, N. H. and Baldwin, L. V., "Decay of Turbulence in Axisymmetric Wakes," *Journal of Basic Engineering*, Vol. 88, March 1966, pp. 261-268.

[9] Tennekes, H. and Lumley, J. L., *A First Course in Turbulence*, MIT Press, Cambridge, Mass., 1972, pp. 104-124.

[10] Castro, I. P., "Wake Characteristics of Two-Dimensional Perforated Plates Normal to an Airstream," *Journal of Fluid Mechanics*, Vol. 46, April 1971, pp. 599-609

[11] Sheldon, G. F., "Measurements of Subsonic Wind Tunnel Performance and Two-Dimensional Turbulent Wake Characteristics," MSCE Thesis, Purdue University, 1980, pp. 1-122.

AIAA 82-4016

Acoustic Oscillations in Internal Cavity Flows: Nonlinear Resonant Interactions

L. King Isaacson* and Alan G. Marshall†
University of Utah, Salt Lake City, Utah

EVIDENCE has been accumulating which indicates that the presence of vortex-driven acoustic oscillations may provide a significant contribution to oscillating pressure levels in segmented solid propellant rocket motors. Several years ago, Flandro and Jacobs[1] suggested that periodic vortex shedding could interact with the chamber acoustics to generate pressure oscillations. Culick and Magiawala[2] were able to produce discrete acoustic oscillations in an open-ended flow cavity using both pairs of obstructions and several obstructions in the flow passage. A recent experimental study by Dunlop and Brown[3] indicated that restrictor pairs placed in a choked internal flow can produce significant increases in the magnitude of the pressure oscillations. Their results indicated that not only is the position of the restrictor pair relative to the acoustic mode structure an important parameter, but that the restrictor spacing is also of importance in determining the pressure oscillations produced by vortex shedding and interaction.

This Note presents experimental results which indicate that, for a fixed restrictor pair location and for a fixed restrictor spacing, the primary acoustic oscillation is produced by vortex interaction with the downstream restrictor pair and that significant nonlinear coupling occurs between the internal shear layers produced by the forward restrictor pair and the acoustic pressure field, resulting in resonant acoustic trios of frequency.

The facility used for this study was a subsonic wind tunnel with a test section 2.44 m in length and a cross section of 17.8×17.8 cm. The internal flow cavity consisted of two sets of restrictor pairs as indicated in Fig. 1. The forward plane of the flow cavity was located at a position 79% of the test section length from the entrance to the test section. An X-configuration, constant-temperature, hot-film anemometer system was used to measure axial velocity frequency spectra for various centerline velocities. Two TSI Model 1050 Constant Temperature Anemometers with two TSI Model 1055 Linearizers, together with a TSI Model 1015C Sum and Difference Circuit were used for the velocity measurements. Frequency spectra were obtained with a Hewlett-Packard Model 3590A Wave Analyzer. Analog data acquisition and digital processing were accomplished with a Hewlett-Packard Model 2240A Measurement and Control Processor, a Hewlett-Packard HP-85 Controller, and a Hewlett-Packard Model 7225A Plotter. Figure 2 shows the velocity frequency spectrum for a cavity centerline velocity of 17.6 m/s. The anemometer sensors were located on the cavity centerline directly between the edges of the forward restrictors.

As the velocity is increased, a variety of acoustic frequencies are produced. Figure 3 presents Strouhal number vs flow Reynolds number where the Strouhal number is defined as

$$S = fL/U_0 \tag{1}$$

where f is the frequency, L the length between restrictor pairs, and U_0 the velocity on the centerline between the edges of the forward restrictor pair. Reynolds number is defined as

$$R = U_0 D/\nu \tag{2}$$

where D is the separation distance between the edges of the forward pair of restrictors and ν the kinematic viscosity. Two broad categories of Strouhal number around the values 1 and 2 are readily apparent. However, specific patterns of Strouhal number of each Reynolds number are also apparent. Figure 4 shows a velocity frequency spectrum for a flow Reynolds number of 7.14×10^4 indicating the frequencies giving rise to the corresponding Strouhal numbers in Fig. 3. Note in Fig. 4 that the frequencies fall into the pattern

$$f_1 \pm f_2 \pm f_3 = 0 \tag{3}$$

There are over 20 sets of Strouhal number in Fig. 3 which fit into this pattern.

This type of relationship reflects a condition of resonance produced by a nonlinear quadratic interaction between the various modes of discrete oscillations. The upper and lower shear layers serve as sources of oscillation energy coupling to the pressure wave equation for the inviscid flow along the

Received June 4, 1981.

*Professor, Dept. of Mechanical and Industrial Engineering. Associate Fellow AIAA.

†Graduate Research Assistant, Dept. of Mechanical and Industrial Engineering.

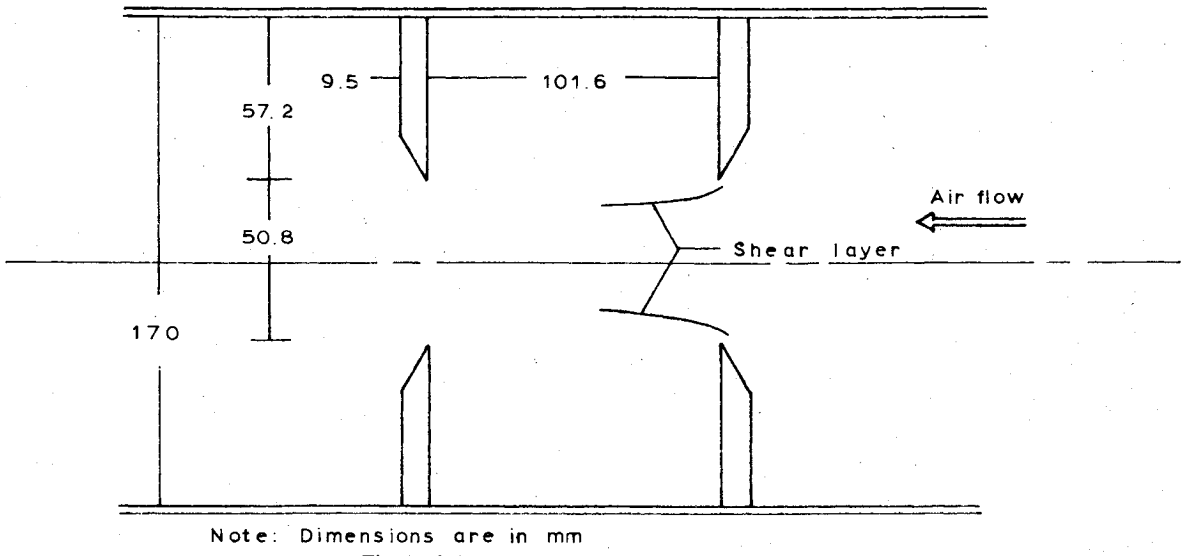

Fig. 1 Schematic diagram of internal flow cavity.

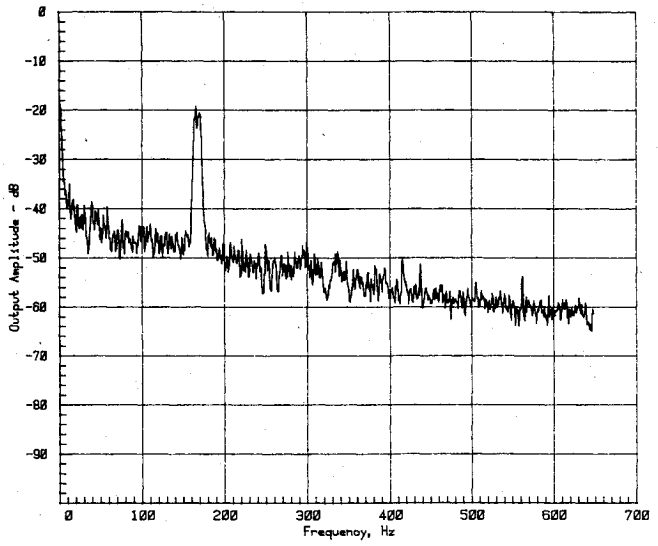

Fig. 2 Velocity frequency spectrum for the axial velocity on the cavity centerline between the edges of the forward restrictors (velocity = 17.6 m/s, $Re = 5.03E+004$).

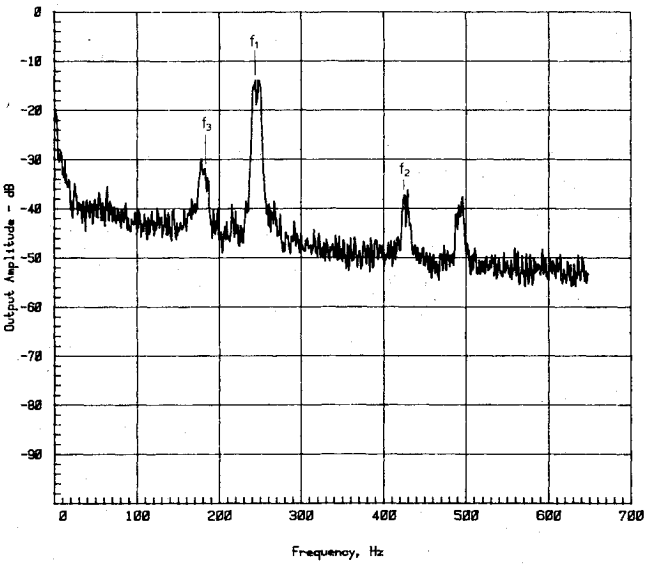

Fig. 4 Velocity frequency spectrum for axial velocity at 25 m/s, $Re = 7.14E+004$.

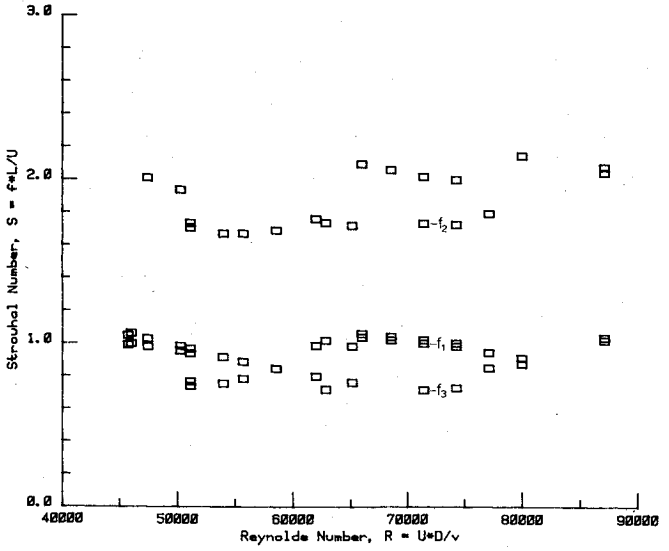

Fig. 3 Strouhal number vs Reynolds number, with the velocity sensors on the cavity centerline between the edges of the forward restrictors.

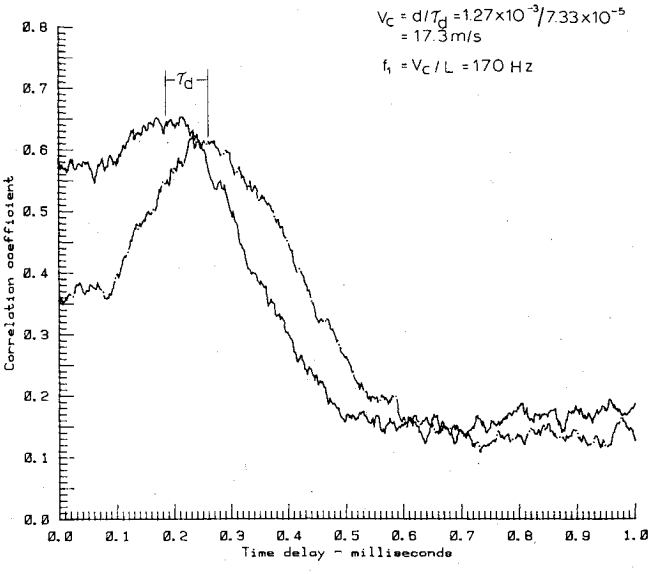

Fig. 5 Time-delay cross-correlation (separation distance d is 1.27 mm, axial flow velocity on the cavity centerline is 17.6 m/s.)

center of the cavity. The early work describing the shear layers as fluid sounding boards was done by Lighthill,[4,5] Phillips,[6] and Landahl.[7] The nonlinear resonance coupling of a quadratic nature leading to resonance of the type indicated in Eq. (3) has been developed by Benney[8] and Bretherton.[9] Recent discussions have been presented by Whitham[10] and Kim et al.[11]

These results indicate that in addition to restrictor spacing and location relative to the acoustic modes of the overall flow system, the presence of amplifying shear layers and reflecting surfaces can produce resonant acoustic energy flows into other frequencies governed by selection rules of the type indicated in Eq. (3).

To determine the source of the primary discrete frequency, such as that indicated in Fig. 2, time-delay cross-correlation measurements were carried out for a single sensor and an X-configuration probe located in the upper shear layer. These results are indicated in Fig. 5. Phillips[6] and Flandro[12] have shown that for vortex production in shear layers, the frequency produced in the acoustic cavity is related to the convective velocity of such vortex structures along the shear layer. From Fig. 5, the convective velocity was determined as approximately 74% of the local shear layer velocity, which resulted in a local convective velocity almost equal to the freestream velocity on the centerline at the forward edge of the cavity. These results yielded a frequency as

$$f = V_c/L = 17.33/0.102 = 170 \text{ Hz} \quad (4)$$

which is the frequency obtained from the spectrum in Fig. 2.

To summarize, these results indicate that significant nonlinear resonant energy transfer of a quadratic nature may be present in internal cavity flows at flow conditions such that the nonlinear frequency selection rules are satisfied. In addition, the primary discrete oscillations produced in such cavity flows have frequencies that are equal in value to the convective velocities of the vortex structures produced in the shear layers divided by the cavity length.

Acknowledgments

The authors wish to gratefully acknowledge support for this project from the University of Utah Research Fund. In addition, many valuable discussions have been held with Prof. Gary A. Flandro, whose assistance is greatly appreciated.

References

[1] Flandro, G. A. and Jacobs, H. A., "Vortex-Generated Sound in Cavities," *Progress in Astronautics and Aeronautics: Aeroacoustics: Jet and Combustion Noise; Duct Acoustics*, Vol. 37, edited by H. T. Nagamatsu, AIAA, New York, 1975, pp. 521-533.

[2] Culick, F.E.C. and Magiawala, K., "Excitation of Acoustic Modes in a Chamber by Vortex Shedding," *Journal of Sound and Vibration*, Vol. 64, No. 3, June 1979, pp. 455-457.

[3] Dunlop, R. and Brown, R. S., "Exploratory Experiments on Acoustic Oscillations Driven by Periodic Vortex Shedding," *AIAA Journal*, Vol. 19, March 1981, pp. 408-409.

[4] Lighthill, M. J., "On Sound Generated Aerodynamically: I. General Theory," *Proceedings of the Royal Society*, Series A, Vol. 211, March 1952, pp. 564-587.

[5] Lighthill, M. J., "On Sound Generated Aerodynamically: II. Turbulence as a Source of Sound," *Proceedings of the Royal Society*, Series A, Vol. 222, Feb. 1954, pp. 1-32.

[6] Phillips, O. M., "On the Generation of Sound by Supersonic Turbulent Shear Layers," *Journal of Fluid Mechanics*, Vol. 9, Pt. 1, Sept. 1960, pp. 1-28.

[7] Landahl, M. T., "A Wave-Guide Model for Turbulent Shear Flows," NASA CR-317, 1965.

[8] Benney, D. J., "Non-Linear Gravity Wave Interactions," *Journal of Fluid Mechanics*, Vol. 14, Pt. 4, Dec. 1962, pp. 577-584.

[9] Bretherton, F. P., "Resonant Interactions Between Waves. The Case of Discrete Oscillations," *Journal of Fluid Mechanics*, Vol. 20, Pt. 3, Nov. 1964, pp. 457-479.

[10] Whitham, G. B., *Linear and Nonlinear Waves*, John Wiley & Sons, New York, 1974, pp. 527-532.

[11] Kim, Y. C., Beall, J. M., Powers, E. J., and Miksad, R. W., "Bispectrum and Nonlinear Wave Coupling," *Physics of Fluids*, Vol. 23, Feb. 1980, pp. 258-263.

[12] Flandro, G. A., "Analytical Studies of the Excitation of Acoustic Waves by Vortex Shedding," *Vortex Shedding Studies*, edited by R. S. Brown et al., AFRPL TR-80-13, April 1980, pp. 88-115.

AIAA 81-0375R

Space Measurements of Tropospheric Aerosols

M. Griggs*
Science Applications, Inc., La Jolla, Calif.

Introduction

THE use of satellite radiance measurements to determine the atmospheric aerosol optical thickness has been under investigation for several years.[1-3] It has been shown that, over ocean surfaces, a linear relationship exists between the upwelling radiance in the visible regions and the aerosol content. The aerosol content is defined in terms of the Elterman[4] model vertical aerosol optical thickness, i.e., the aerosol content is given by the ratio (measured aerosol optical thickness at wavelength λ to a model aerosol optical thickness at wavelength λ) $\times N$. That is, a value of $2N$ for the aerosol content indicates that the optical thickness is twice that of the Elterman model. In the results reported here, measurements of the aerosol optical thickness were available only at 0.5 μm, so that all radiances measured by the different radiometers are plotted against aerosol content, where N indicates an aerosol optical thickness of 0.213 (the Elterman model value) measured at 0.5 μm.

Linear relationships between the upwelling radiance and the aerosol content have been determined for Landsat 1,[1] Landsat 2,[2] NOAA-5,[3] GOES-1,[3] and SMS-2. A global-scale ground-truth experiment using NOAA-6 data was conducted in 1980 to investigate the variability of the linear relationship at different sites around the globe; no results are yet available. The possibility of using this ocean technique over inland bodies of water such as rivers, lakes, and reservoirs has been investigated using Landsat 2 data.

Ocean Data

The relationships between radiance and the aerosol content are found to be different for each satellite. This can be due to the aerosol properties being different for each data set or due to uncertainties in the radiometric calibrations of the satellite sensors. The Landsat study[5] found evidence of radiometric calibration differences between Landsat 1 and Landsat 2, and it is believed that similar calibration problems are mainly responsible for the differences in the results given below.

Landsat Results

Data have been obtained at several sites for Landsat overpasses,[5] the largest data set being for the Pacific Ocean at San Diego for Landsat 2 overpasses. These results are shown

Presented as Paper 81-0375 at the AIAA 19th Aerospace Sciences Meeting, St. Louis, Mo., Jan. 12-15, 1981; submitted March 6, 1981; revision received Aug. 3, 1981.

*Senior Scientist, Electronic Vision & Systems Division.